

Ateneo de Manila University

Archium Ateneo

---

Environmental Science Faculty Publications

Environmental Science Department

---

2-2021

## Determination of Photon Shielding Parameters for Soils in Mangrove Forests

Frederick C. Hila

*University of the Philippines Diliman*

Gerald P. Dicen

*Department of Science and Technology Philippine Nuclear Research Institute (DOST-PNRI)*

Abigaile Mia V. Javier-Hila

*Department of Science and Technology Philippine Nuclear Research Institute (DOST-PNRI)*

Alvie Asuncion-Astronomo

*Department of Science and Technology Philippine Nuclear Research Institute (DOST-PNRI)*

Neil Raymund D. Guillermo

*Department of Science and Technology Philippine Nuclear Research Institute (DOST-PNRI)*

*See next page for additional authors*

Follow this and additional works at: <https://archium.ateneo.edu/es-faculty-pubs>



Part of the [Environmental Sciences Commons](#), and the [Soil Science Commons](#)

---

### Custom Citation

Hila, F. C., Dicen, G. P., Javier-Hila, A. M. V., Asuncion-Astronomo, A., Guillermo, N. R. D., Rallos, R. V., Navarrete, I. A., & Amorsolo, A. V. Jr. (2021). Determination of photon shielding parameters for soils in mangrove forests. *Philippine Journal of Science*, 150(1), 245–256. <https://philjournalsci.dost.gov.ph/publication/regular-issues/past-issues/102-vol-150-no-1-february-2021/1300-determination-of-photon-shielding-parameters-for-soils-in-mangrove-forests>

This Article is brought to you for free and open access by the Environmental Science Department at Archium Ateneo. It has been accepted for inclusion in Environmental Science Faculty Publications by an authorized administrator of Archium Ateneo. For more information, please contact [oadrcw.ls@ateneo.edu](mailto:oadrcw.ls@ateneo.edu).

---

**Authors**

Frederick C. Hila, Gerald P. Dicen, Abigaile Mia V. Javier-Hila, Alvie Asuncion-Astronomo, Neil Raymund D. Guillermo, Roland V. Rallos, Ian A. Navarrete, and Alberto V. Amorsolo Jr

## Determination of Photon Shielding Parameters for Soils in Mangrove Forests

Frederick C. Hila<sup>1,2\*</sup>, Gerald P. Dicen<sup>2</sup>, Abigaile Mia V. Javier-Hila<sup>2</sup>,  
Alvie Asuncion-Astronomo<sup>2</sup>, Neil Raymund D. Guillermo<sup>2</sup>, Roland V. Rallos<sup>2</sup>,  
Ian A. Navarrete<sup>3,4</sup>, and Alberto V. Amorsolo Jr.<sup>5</sup>

<sup>1</sup>Materials Science and Engineering Program, College of Engineering  
University of the Philippines Diliman, Quezon City 1101 Metro Manila, Philippines

<sup>2</sup>Department of Science and Technology  
Philippine Nuclear Research Institute (DOST-PNRI)  
Commonwealth Avenue, Diliman, Quezon City 1101 Metro Manila, Philippines

<sup>3</sup>Department of Environmental Science, School of Science and Engineering  
Ateneo de Manila University, Loyola Heights  
Quezon City 1108 Metro Manila, Philippines

<sup>4</sup>Department of Environmental Science, Southern Leyte State University  
Hinunangan Campus 6608 Southern Leyte, Philippines

<sup>5</sup>Department of Mining, Metallurgical and Materials Engineering, College of Engineering  
University of the Philippines Diliman, Quezon City 1101 Metro Manila, Philippines

**The mass attenuation coefficient (MAC), effective atomic number ( $Z_{\text{eff}}$ ), and effective electron density ( $N_{\text{eff}}$ ) values of soils in mangrove forests across the Philippine islands were investigated. In addition, ENDF/B-VI.8 cross-section data library was used for interpolating  $Z_{\text{eff}}$  and  $N_{\text{eff}}$  values. Photon energies considered in this study ranged from 59.5–1332 keV. MAC values were obtained using MCNP5 and PHITS Monte Carlo (MC) simulations and were found to be in good agreement with XCOM and values in literature. Results for  $Z_{\text{eff}}$  were in good agreement with values obtained using Phy-X/ZEXTRA program. Each shielding parameter was investigated as a function of  $\text{SiO}_2$  concentrations.**

Keywords: effective atomic number, gamma ray, mass attenuation coefficient, silica,  $\text{SiO}_2$ , soil

### INTRODUCTION

Photon attenuation parameters – including the MAC,  $Z_{\text{eff}}$ , and  $N_{\text{eff}}$  – are important quantities that have been subjects of interest for a wide range of materials, including natural matter such as rocks (Obaid *et al.* 2018a; Alorfi *et al.* 2020), concretes (Mahmoud *et al.* 2019a), ores (Un and Sahin 2011), and minerals (Agar *et al.* 2019;

Han *et al.* 2009). These quantities have been used for acquiring important characteristics of soils such as bulk density, water retention, porosity, and particle sizes in a non-invasive and accurate manner (Mudahar and Sahota 1988a; Pires 2018; Elias 2004). On the other hand, MAC values of soils are also used for self-correction factors essential in gamma spectrometry of many geological and environmental samples (Al-Masri *et al.* 2013).

\*Corresponding Author: fchila@pnri.dost.gov.ph

Soils are additionally recognized as highly abundant, cheap, and effective radiation shielding media (Mudahar and Sahota 1988a). They are composed of both organic and inorganic matter, with silica ( $\text{SiO}_2$ ) as typically the largest component. Thus, shielding parameters of soils have been investigated for a variety of types and origins (Mudahar and Sahota 1988b; Un and Sahin 2012; Kucuk *et al.* 2013; Sayyed *et al.* 2019). For photon shielding, the  $Z_{\text{eff}}$  and  $N_{\text{eff}}$  are convenient parameters for composite materials and can both be derived from measured MAC values, which are dependent on photon energy.

For the determination of attenuation coefficients of multi-element materials, numerous studies have used MC simulations due to its versatility, accuracy, and capability to consider the effects of geometry. This method is done by modeling a narrow-beam setup inclusive of the collimator and detector (Divina *et al.* 2020; Boukhris *et al.* 2020; Al-Hadeethi *et al.* 2020). This method has been previously used in acquiring attenuation coefficients for natural and building materials – including selected rocks, concretes, bricks, and minerals (Obaid *et al.* 2018b, c; Mahmoud *et al.* 2019b; Sharifi *et al.* 2013; Singh *et al.* 2018; Medhat 2015). It was also recently used for acquiring the attenuation coefficients of soils from chosen locations in Egypt (Akar Tarim *et al.* 2013; Medhat *et al.* 2014) and in Iraq (Taqi and Khalil 2017).

The primary objective of this study is to obtain MAC,  $Z_{\text{eff}}$ , and  $N_{\text{eff}}$  values of soil samples specifically collected from Philippine mangrove forests. The MCNP5 and PHITS MC codes were used to obtain MAC values, which were compared with XCOM. The results obtained were interpolated to determine  $Z_{\text{eff}}$  and  $N_{\text{eff}}$  values. The

photoatomic library for interpolations was the pooled ENDF/B-VI.8 previously extracted for the construction of a photon shielding program (Hila *et al.* 2020). This particular library is appropriate since it is the exact library used by the MC simulation codes. Results of  $Z_{\text{eff}}$  and  $N_{\text{eff}}$  values were compared by using the Phy-X/ZEXTRA (Özpolat *et al.* 2020), which uses the pooled WinXCom (Gerward *et al.* 2001, 2004) photon cross-section database taken from XCOM. Furthermore, the effect of the silica amount on the attenuation parameters was investigated by Akar Tarim *et al.* (2013) and is also investigated in this work.

## MATERIALS AND METHODS

### Soil Sampling and Analysis

Five areas across the Philippine islands were selected for this study (Figure 1). Sampling locations include Zambales (Masinloc and Subic), Palawan (Bogtong and Calauit), and Cebu (Kodia). All sampling locations are natural mangrove forests. The nature of the sites and morphology of the mangrove soils are described in the previous study (Dicen *et al.* 2019).

Mangrove soil sediments were collected using a corer with a length of 100 cm and a diameter of 6.5 cm. Samples were subdivided into two sampling depths (0–40 cm, 40–100 cm). The exception is for Kodia soils (0–40 cm, 40–75 cm), which had a shallow soil layer. Large particles were removed by sieving through a 0.5-mm sieve. Samples were ground and oven-dried for 20 h at 150 °C. These were placed in an aluminum disc and pelletized using

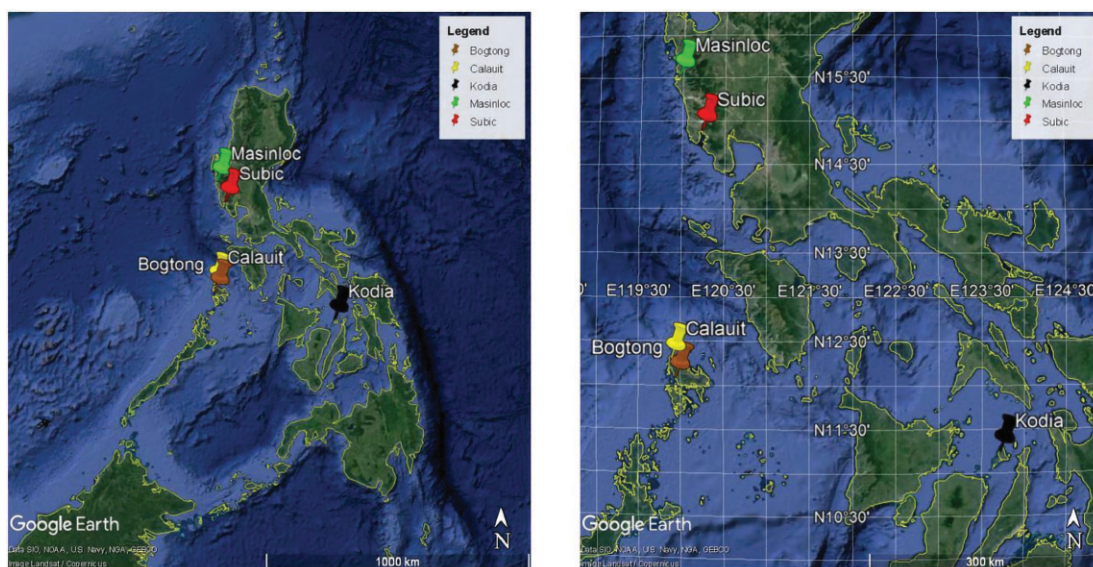


Figure 1. Soil sampling sites taken using Google Earth Pro.

a 10-ton hydraulic press. Semi-quantitative elemental analysis of each sample was accomplished using a hand-held Olympus XRF analyzer.

### Theory

Under narrow beam conditions, the relationship between photon transmission and MAC  $\mu/\rho$  (in  $\text{cm}^2\text{g}^{-1}$ ) for any material is given by Beer-Lambert law shown in Equation 1.

$$I = I_0 \exp\left(-\left(\frac{\mu}{\rho}\right) \rho x\right) \quad (1)$$

For this equation,  $I_0$  and  $I$  are the incident and transmitted beam intensities, respectively,  $\rho$  is the density (in  $\text{g}/\text{cm}^3$ ),  $\mu$  is the linear attenuation coefficient (in  $\text{cm}^{-1}$ ), and  $x$  is the material or absorber thickness (in cm).

For compounds and mixtures,  $\mu/\rho$  is given by the mixture rule in Equation 2, where  $w_i$  is the weight fraction of the  $i^{\text{th}}$  element.

$$\frac{\mu}{\rho} = \sum_i w_i \left(\frac{\mu}{\rho}\right)_i \quad (2)$$

Moreover, the MAC is proportional to the total atomic cross-section  $\sigma_T$  (in  $\text{cm}^2 \text{atom}^{-1}$ ) shown in Equation 3, where  $N_A$  is Avogadro's number,  $n_i$  is the number of atoms in the molecular formula, and  $A_i$  is the corresponding atomic mass of the  $i^{\text{th}}$  atom. The term  $\sum_i n_i$  is the total number of atoms in the molecular formula and the  $\sum_i n_i A_i$  is the molecular mass.

$$\sigma_T = \frac{\sum n_i A_i}{N_A \sum n_i} \left(\frac{\mu}{\rho}\right) \quad (3)$$

On the other hand,  $Z_{\text{eff}}$  and  $N_{\text{eff}}$  are highly used quantities for characterizing shielding properties (Monisha *et al.* 2020). These are also used in the calculations of doses for radiation therapy and in agricultural industries (Akman *et al.* 2015).  $Z_{\text{eff}}$  is a dimensionless quantity and can be obtained by logarithmic interpolation of elemental cross-sections shown in Equation 4 (Singh *et al.* 2007), where  $\sigma_1$  and  $\sigma_2$  are elemental cross-sections that bound the value of  $\sigma_T$ , while  $Z_1$  and  $Z_2$  are the corresponding atomic numbers of the elements. The  $N_{\text{eff}}$  (in electrons/g) is related to  $Z_{\text{eff}}$  and is calculated using Equation 5.

$$Z_{\text{eff}} = \frac{Z_1(\log \sigma_2 - \log \sigma_T) + Z_2(\log \sigma_T - \log \sigma_1)}{\log \sigma_2 - \log \sigma_1} \quad (4)$$

$$N_{\text{eff}} = \frac{N_A}{A_i} Z_{\text{eff}} \sum_i n_i \quad (5)$$

### MC Simulations

For this study, MCNP5 (X-5 Monte Carlo Team 2008) and PHITS (Sato *et al.* 2018) MC codes were used to

obtain the MAC values. Both codes use photoatomic data libraries based on EPDL97, which is the photon library of the ENDF/B-VI.8. In this study, both simulation codes were used to model the narrow-beam geometry shown in Figure 2.

Mangrove soil samples were modeled at 15 cm from the detector surface. Sample lengths were adjusted per photon energy such that Nordfors criteria ( $2 \leq \ln(I_0/I) \leq 4$ ) is satisfied. The lead collimator was modeled with a hole diameter of 4 mm and a thickness of 5 cm. The detector cell was composed of a  $3 \times 3$  in NaI(Tl) crystal.

The source was modeled as a planar disk emitting a collimated beam of monoenergetic photons. The photon energies of interest were from the gamma photons from  $^{241}\text{Am}$  (59.5 keV),  $^{133}\text{Ba}$  (81, 303, 356 keV),  $^{109}\text{Cd}$  (88 keV),  $^{57}\text{Co}$  (122, 136 keV),  $^{60}\text{Co}$  (1173, 1332 keV),  $^{137}\text{Cs}$  (662 keV),  $^{54}\text{Mn}$  (835 keV), and  $^{22}\text{Na}$  (1275 keV).

In both MC simulation codes, the average cell fluence tallies were used. In MCNP5, this pertains to the F4 tally, while in PHITS the [T-Track] tally. Energy binning was implemented to obtain the relative fluences from uncollided photons. All MC simulations were accomplished at an amount of  $10^7$  generated source photons per photon energy.

### $Z_{\text{eff}}$ Using ENDF/B-VI.8

For obtaining the  $Z_{\text{eff}}$  values using Equation 4, an elemental cross-section database is required and is typically the XCOM-NIST library. In this study, the EPDL97 (ENDF/B-VI.8) photoatomic library from LLNL was used. This library can be obtained in ENDF-6 format from IAEA-NDS; otherwise, it can be extracted from the ACE data files of each simulation code or printed using MCNP5 XS plotting command. The element libraries extracted in ENDF-6 format was used in this work. The details of the extraction are described by Hila *et al.* (2020). Total cross-sections were stored in an MS Excel spreadsheet for automatic interpolations using Equation 4 via a VBA-based script.  $Z_{\text{eff}}$  values were used subsequently to obtain  $N_{\text{eff}}$  values.

### XCOM and Phy-X/ZEXTRA

The XCOM (Berger *et al.* 1998) is a widely used database for obtaining MAC values for multi-element materials. It uses interpolations of the elemental MAC values (or elemental cross-sections) at specified energies and applies the mixture rule based on the specified compositions. Total MAC values are interpolated by XCOM using a log-log cubic spline fit.

The Phy-X/ZEXTRA (Özpolat *et al.* 2020) is a new web program for calculating  $Z_{\text{eff}}$  values for photons, electrons,

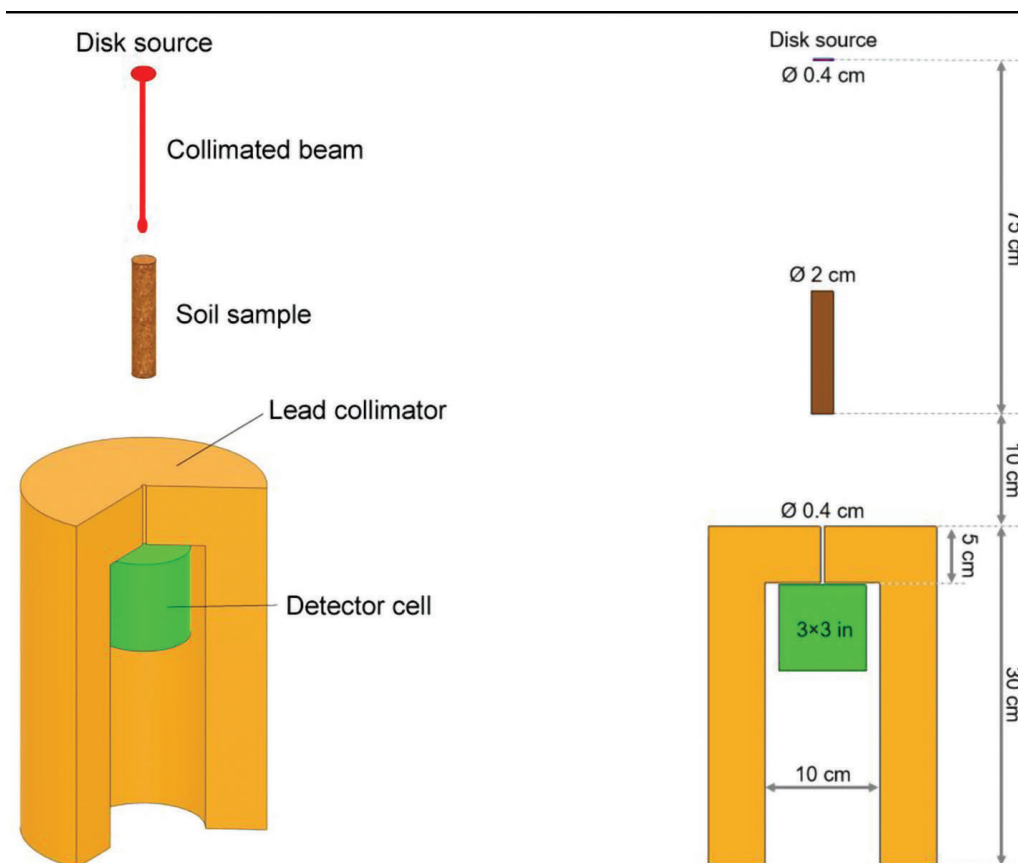


Figure 2. Setup for acquiring the MAC values of mangrove soil samples.

protons, alpha particles, and carbon ions. For photons, this program uses the cross-section libraries from the WinXCom (Gerward *et al.* 2001, 2004). This program is similar in interface to the new Phy-X/PSD (Şakar *et al.* 2020). However, it differs in the calculated  $Z_{\text{eff}}$  values since Phy-X/ZeXTRA is based on logarithmic interpolation of elemental cross-sections shown in Equation 4. Therefore, it is the appropriate software for comparison in this work.

## RESULTS AND DISCUSSION

The XRF elemental analysis of the various mangrove soils in the Philippines is shown in Table 1. Based on these compositions, the MAC values were derived *via* the MC method using MCNP5 and PHITS, with results shown in Table 2. These revealed a good agreement between both MC codes since both codes use identical photoatomic libraries based on EPDL97. These results were also in agreement with XCOM values and with those described in the literature (Akman *et al.* 2019; Costa *et al.* 2013; Taqi *et al.* 2016; Appoloni and Rios 1994; Alam *et al.*

2001; Medhat 2012). Furthermore, small disagreements between XCOM and MC simulations are attributed to both the slight deviation from narrow beam geometry and the difference in the cross-section libraries of XCOM and EPDL97.

The tabulated MAC values from MCNP5 are plotted as a function of  $\text{SiO}_2$  concentrations shown in Figure 3a. For the lower energy regions, the smallest values for attenuation coefficients are from the Calauit region, which inversely has the largest concentrations of  $\text{SiO}_2$ . On the other hand, the mangrove soils from Kodia and Subic have lower  $\text{SiO}_2$  concentrations and conversely have the largest coefficient values. This was also observed by Akar Tarim *et al.* (2013) in Egyptian soils from agricultural zones.

The effect of soil composition in attenuation coefficients is found to be less pronounced at energies above 300 keV where the primary interaction mechanism is through Compton interactions. This is in congruence with Mudahar and Sahota (1988a) and Appoloni and Rios (1994).

Moreover, for the  $Z_{\text{eff}}$  values, results for the different Philippine mangrove soils are shown in Table 3. These values are displayed in Figure 3b as a function of  $\text{SiO}_2$

**Table 1.** Compositions (%wt) of Philippine soils found in mangrove forests at different locations and depths.

Component	Bogtong		Calauit		Kodia		Masinloc		Subic	
	Surface [0–40 cm]	Sub [40–100 cm]	Surface [0–40 cm]	Sub [40–100 cm]	Surface [0–40 cm]	Sub [40–75 cm]	Surface [0–40 cm]	Sub [40–100 cm]	Surface [0–40 cm]	Sub [40–100 cm]
O	51.26	51.19	51.84	50.61	44.15	44.47	47.95	47.24	46.95	44.50
Si	30.11	32.23	38.97	34.42	16.28	14.06	25.76	22.47	24.17	19.32
Al	4.02	4.20	3.67	5.99	9.22	8.40	8.19	8.08	12.04	12.61
Ca	0.09	0.02	<0.01	<0.01	13.79	12.64	4.56	4.43	2.46	1.49
Fe	2.61	2.48	1.08	2.15	5.68	5.94	4.28	5.10	8.03	13.94
Mg	2.57	2.13	1.69	2.52	3.65	3.70	4.68	4.82	3.88	3.40
S	5.48	4.00	1.13	1.08	3.62	5.24	2.49	3.20	1.05	0.84
Ti	3.61	3.51	1.44	2.95	2.80	4.93	1.44	4.01	0.68	2.65
Zr	0.18	0.18	0.17	0.25	0.53	0.42	0.47	0.46	0.58	1.00
P	0.02	0.02	<0.01	<0.01	<0.01	0.06	0.03	0.04	0.05	0.03
Sr	0.02	0.02	<0.01	0.02	0.07	0.06	0.06	0.07	0.08	0.09
Mn	0.02	0.02	0.02	0.02	0.03	0.02	0.02	0.02	0.02	0.01
Silica	64.42	68.96	83.37	73.63	34.83	30.07	55.11	48.07	51.71	41.33

**Table 2.** Mass attenuation coefficients ( $\text{cm}^2\text{g}^{-1}$ ) of Philippine mangrove soils at different energies, obtained by MCNP5, PHITS, XCOM, and experiments in the literature.

Energy (keV)	Bogtong surface [0–40 cm]			Bogtong sub [40–100 cm]			Calauit surface [0–40 cm]			Calauit sub [40–100 cm]		
	MCNP5	PHITS	XCOM	MCNP5	PHITS	XCOM	MCNP5	PHITS	XCOM	MCNP5	PHITS	XCOM
59.5	0.3047	0.3046	0.3050	0.3019	0.3017	0.3021	0.2761	0.2759	0.2764	0.2958	0.2956	0.2961
81.0	0.2116	0.2116	0.2119	0.2105	0.2104	0.2108	0.2004	0.2004	0.2007	0.2081	0.2081	0.2084
88.0	0.1965	0.1964	0.1969	0.1956	0.1955	0.1961	0.1878	0.1878	0.1883	0.1937	0.1937	0.1942
122	0.1579	0.1579	0.1582	0.1576	0.1576	0.1579	0.1549	0.1548	0.1552	0.1569	0.1569	0.1572
136	0.1490	0.1489	0.1494	0.1487	0.1487	0.1491	0.1469	0.1468	0.1472	0.1482	0.1482	0.1486
303	0.1067	0.1067	0.1070	0.1067	0.1067	0.1069	0.1067	0.1067	0.1070	0.1066	0.1066	0.1069
356	0.0999	0.0999	0.1002	0.0999	0.0999	0.1002	0.1000	0.1000	0.1003	0.0998	0.0998	0.1001
662	0.0766	0.0767	0.0769	0.0766	0.0767	0.0769	0.0768	0.0768	0.0771	0.0766	0.0766	0.0769
835	0.0688	0.0688	0.0690	0.0688	0.0688	0.0691	0.0690	0.0690	0.0692	0.0688	0.0688	0.0690
1173	0.0582	0.0582	0.0584	0.0582	0.0583	0.0585	0.0584	0.0584	0.0586	0.0582	0.0582	0.0584
1275	0.0559	0.0559	0.0560	0.0559	0.0559	0.0560	0.0560	0.0560	0.0562	0.0558	0.0559	0.0560
1332	0.0546	0.0546	0.0548	0.0546	0.0546	0.0548	0.0547	0.0547	0.0549	0.0546	0.0546	0.0548

Energy (keV)	Kodia surface [0–40 cm]			Kodia sub [40–75 cm]			Masinloc surface [0–40 cm]			Masinloc sub [40–100 cm]		
	MCNP5	PHITS	XCOM	MCNP5	PHITS	XCOM	MCNP5	PHITS	XCOM	MCNP5	PHITS	XCOM
59.5	0.4004	0.4002	0.4006	0.4009	0.4006	0.4011	0.3369	0.3367	0.3372	0.3569	0.3567	0.3572
81.0	0.2500	0.2499	0.2503	0.2498	0.2498	0.2501	0.2246	0.2246	0.2250	0.2324	0.2324	0.2328
88.0	0.2264	0.2263	0.2269	0.2262	0.2261	0.2266	0.2067	0.2066	0.2071	0.2127	0.2126	0.2131
122	0.1712	0.1711	0.1715	0.1688	0.1688	0.1692	0.1622	0.1622	0.1625	0.1643	0.1643	0.1647
136	0.1585	0.1584	0.1589	0.1567	0.1566	0.1571	0.1520	0.1520	0.1524	0.1535	0.1534	0.1539

Energy (keV)	Kodia surface [0–40 cm]			Kodia sub [40–75 cm]			Masinloc surface [0–40 cm]			Masinloc sub [40–100 cm]		
	MCNP5	PHITS	XCOM	MCNP5	PHITS	XCOM	MCNP5	PHITS	XCOM	MCNP5	PHITS	XCOM
303	0.1074	0.1074	0.1077	0.1070	0.1070	0.1073	0.1069	0.1069	0.1072	0.1068	0.1068	0.1071
356	0.1002	0.1002	0.1006	0.1000	0.0999	0.1003	0.1000	0.0999	0.1003	0.0998	0.0998	0.1002
662	0.0765	0.0765	0.0767	0.0764	0.0764	0.0766	0.0766	0.0766	0.0768	0.0764	0.0764	0.0766
835	0.0686	0.0687	0.0689	0.0685	0.0686	0.0688	0.0687	0.0688	0.0690	0.0686	0.0686	0.0688
1173	0.0580	0.0581	0.0583	0.0580	0.0580	0.0582	0.0581	0.0582	0.0584	0.0580	0.0580	0.0582
1275	0.0557	0.0557	0.0559	0.0556	0.0556	0.0558	0.0558	0.0558	0.0560	0.0556	0.0557	0.0558
1332	0.0544	0.0544	0.0546	0.0543	0.0543	0.0545	0.0545	0.0545	0.0547	0.0544	0.0544	0.0546

Energy (keV)	Subic surface [0–40 cm]			Subic sub [40–100 cm]			Range in literature
	MCNP5	PHITS	XCOM	MCNP5	PHITS	XCOM	
59.5	0.3625	0.3623	0.3627	0.4409	0.4406	0.4411	0.239–0.322 <sup>a</sup> ; 0.3562–0.3793 <sup>b</sup> ; 0.243 <sup>c</sup>
81.0	0.2356	0.2356	0.2359	0.2668	0.2667	0.2671	0.181–0.202 <sup>a</sup>
88.0	0.2151	0.2151	0.2156	0.2394	0.2393	0.2398	0.173–0.189 <sup>a</sup>
122	0.1647	0.1647	0.1651	0.1735	0.1735	0.1738	0.140 <sup>g</sup>
136	0.1538	0.1537	0.1541	0.1599	0.1598	0.1603	–
303	0.1067	0.1067	0.1070	0.1068	0.1068	0.1071	0.098–0.106 <sup>e</sup>
356	0.0998	0.0998	0.1001	0.0997	0.0996	0.1000	0.135 <sup>c</sup> ; 0.082–0.096 <sup>d</sup> ; 0.091–0.098 <sup>e</sup>
662	0.0764	0.0764	0.0766	0.0760	0.0760	0.0762	0.0708–0.0773 <sup>b</sup> ; 0.113 <sup>c</sup> ; 0.064–0.074 <sup>d</sup>
835	0.0685	0.0686	0.0688	0.0682	0.0682	0.0684	0.0700 <sup>g</sup>
1173	0.0580	0.0580	0.0582	0.0576	0.0577	0.0579	0.092 <sup>c</sup> ; 0.047–0.054 <sup>d</sup>
1275	0.0556	0.0556	0.0558	0.0553	0.0553	0.0555	–
1332	0.0543	0.0544	0.0545	0.0540	0.0540	0.0542	0.079 <sup>c</sup> ; 0.042–0.049 <sup>d</sup>

<sup>a</sup>Akman et al. (2019); <sup>b</sup>Costa et al. (2013); <sup>c</sup>Taqi et al. (2016); <sup>d</sup>Medhat (2012); <sup>e</sup>Alam et al. (2001); <sup>f</sup>Alam et al. (2001); <sup>g</sup>Appoloni and Rios (1994)

**Table 3.** Z<sub>eff</sub> values of Philippine mangrove soils using MCNP5 and interpolation of cross-sections from the ENDF/B-VI.8.

Energy (keV)	Bogtong		Calait		Kodia		Masinloc		Subic	
	[0–40 cm]	[40–100 cm]	[0–40 cm]	[40–100 cm]	[0–40 cm]	[40–75 cm]	[0–40 cm]	[40–100 cm]	[0–40 cm]	[40–100 cm]
59.5	11.9993	11.9390	11.3557	11.8111	13.9146	13.9417	12.6747	13.0720	13.1348	14.4327
81.0	11.4843	11.4342	10.9513	11.3285	13.2885	13.3113	12.0939	12.4563	12.5272	13.7583
88.0	11.3303	11.2839	10.8364	11.1855	13.0699	13.0918	11.9088	12.2546	12.3159	13.5033
122	10.8323	10.8006	10.4894	10.7323	12.3556	12.2608	11.3007	11.5713	11.5585	12.4855
136	10.7053	10.6774	10.4001	10.6165	12.0946	12.0166	11.1227	11.3692	11.3482	12.1795
303	10.3338	10.3176	10.1473	10.2796	11.2486	11.2545	10.5969	10.7494	10.7043	11.1844
356	10.3078	10.2926	10.1282	10.2558	11.1916	11.2041	10.5625	10.7099	10.6640	11.1195
662	10.2752	10.2611	10.1071	10.2266	11.1055	11.1300	10.5147	10.6539	10.6063	11.0213
835	10.2700	10.2561	10.1031	10.2218	11.0928	11.1190	10.5074	10.6455	10.5976	11.0075
1173	10.2657	10.2518	10.0998	10.2175	11.0819	11.1096	10.5010	10.6383	10.5903	10.9957
1275	10.2711	10.2573	10.1053	10.2231	11.0875	11.1155	10.5064	10.6436	10.5955	11.0008
1332	10.2670	10.2532	10.1013	10.2190	11.0831	11.1114	10.5025	10.6398	10.5917	10.9969

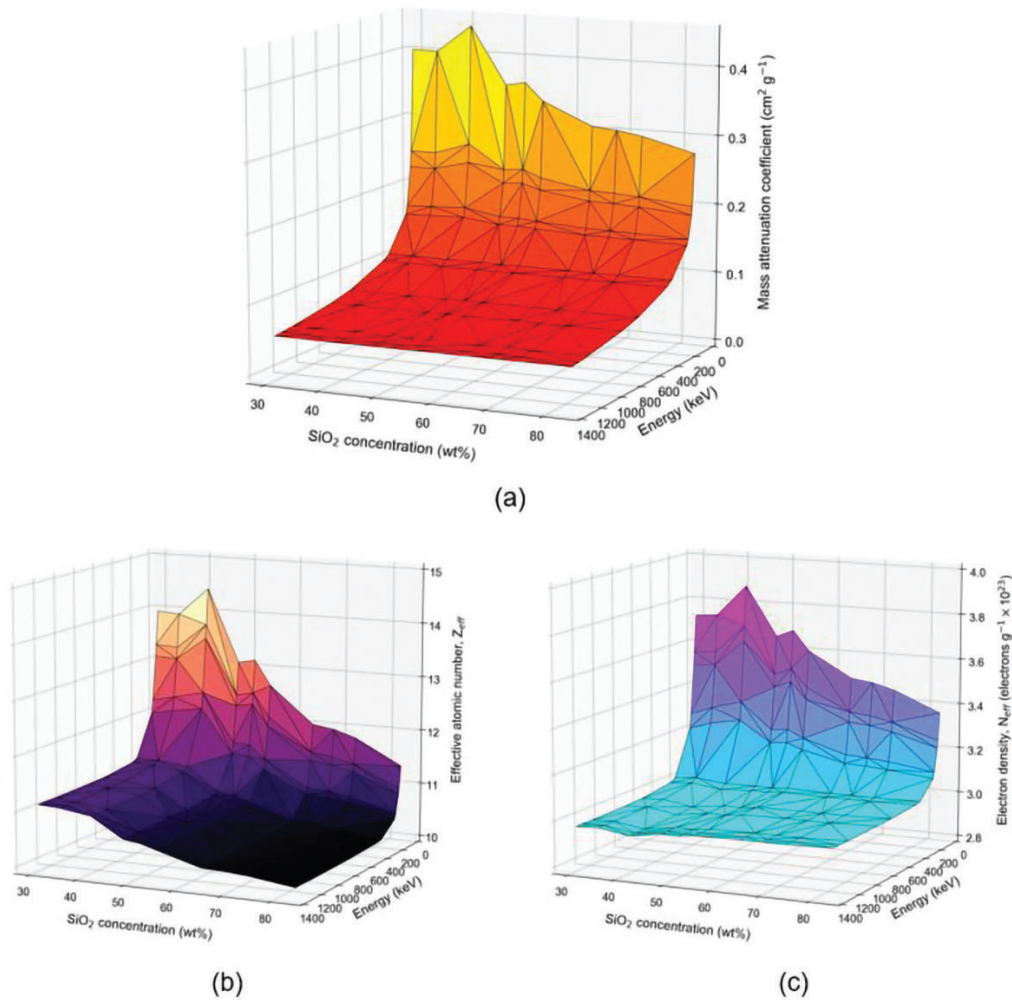


**Figure 3.** Curves of (a) MAC, (b)  $Z_{\text{eff}}$  and (c)  $N_{\text{eff}}$  values based on  $\text{SiO}_2$  concentration of the mangrove soils.

concentrations. Except for the lower energy region and low  $\text{SiO}_2$ , this data shows a negative correlation between the  $Z_{\text{eff}}$  values and the  $\text{SiO}_2$  concentrations. The negative correlation is found even in the higher energy region. This correlation is due to the decreased proportion of heavier oxides with the increase of  $\text{SiO}_2$ . The presence of common heavier oxides such as  $\text{Fe}_2\text{O}_3$  generally leads to increased  $Z_{\text{eff}}$  values.

Subsequently, the  $Z_{\text{eff}}$  values were used to obtain  $N_{\text{eff}}$  values, which are shown in Table 4. These values are displayed as a function of  $\text{SiO}_2$  concentrations in Figure 3c. This figure matches the curve of the MAC values as a function of  $\text{SiO}_2$  concentrations.

$Z_{\text{eff}}$  values obtained in this study were compared with those generated using the Phy-X/ZEXTRA software. The plots shown in Figures 4–8 demonstrate good agreements between the  $Z_{\text{eff}}$  values from this work and Phy-X/ZEXTRA. Notably, the same logarithmic interpolation

method is employed by the Excel VBA based script in this work and the Phy-X/ZEXTRA in obtaining  $Z_{\text{eff}}$ . The only difference is the source of photoatomic libraries, which is the EPDL97 (ENDF/B-VI.8) for the created script.

The initial downward curve found in the energies below 300 keV is due to the dominance of photoelectric interactions. Subsequently, a nearly constant curve is seen in the Compton dominated region. For this region, similar trends were shown by Kucuk *et al.* (2013) for  $Z_{\text{eff}}$  and  $N_{\text{eff}}$  values of Turkish soils.

## CONCLUSION

This work reports the MAC,  $Z_{\text{eff}}$ , and  $N_{\text{eff}}$  values of Philippine mangrove soils obtained from different mangrove forest regions. Photon energies considered ranged from 59.5–1332 keV. MC simulations by both

**Table 4.**  $N_{\text{eff}}$  values (electrons  $\text{g}^{-1} \times 10^{23}$ ) of Philippine mangrove soils.

Energy (keV)	Bogtong		Calauit		Kodia		Masinloc		Subic	
	[0–40 cm]	[40–100 cm]	[0–40 cm]	[40–100 cm]	[0–40 cm]	[40–75 cm]	[0–40 cm]	[40–100 cm]	[0–40 cm]	[40–100 cm]
59.5	3.4900	3.4774	3.3644	3.4508	3.7353	3.7281	3.6002	3.6560	3.6877	3.8764
81.0	3.3402	3.3304	3.2446	3.3098	3.5672	3.5595	3.4352	3.4838	3.5172	3.6953
88.0	3.2954	3.2866	3.2105	3.2680	3.5085	3.5008	3.3826	3.4274	3.4578	3.6268
122	3.1505	3.1458	3.1077	3.1356	3.3168	3.2786	3.2099	3.2363	3.2452	3.3534
136	3.1136	3.1099	3.0813	3.1018	3.2467	3.2133	3.1593	3.1798	3.1861	3.2712
303	3.0055	3.0051	3.0063	3.0034	3.0196	3.0095	3.0100	3.0064	3.0054	3.0040
356	2.9980	2.9979	3.0007	2.9964	3.0043	2.9960	3.0002	2.9954	2.9940	2.9865
662	2.9885	2.9887	2.9944	2.9879	2.9812	2.9762	2.9866	2.9797	2.9778	2.9602
835	2.9870	2.9872	2.9932	2.9865	2.9778	2.9733	2.9846	2.9774	2.9754	2.9565
1173	2.9857	2.9860	2.9923	2.9852	2.9749	2.9707	2.9827	2.9754	2.9734	2.9533
1275	2.9873	2.9876	2.9939	2.9869	2.9764	2.9723	2.9843	2.9768	2.9748	2.9547
1332	2.9861	2.9864	2.9927	2.9857	2.9752	2.9712	2.9832	2.9758	2.9737	2.9536

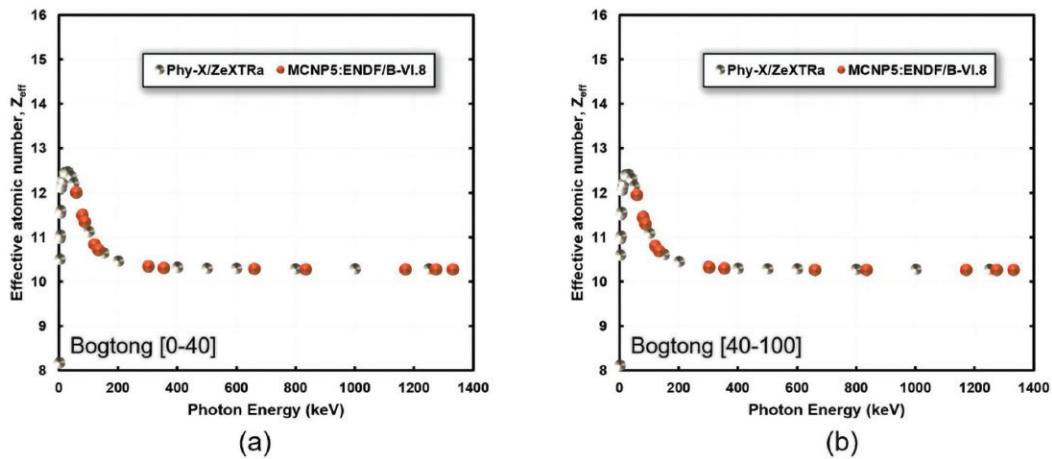


**Figure 4.**  $Z_{\text{eff}}$  values of mangrove soils from Bogtong using MCNP5 and ENDF/B-VI.8 cross-sections and Phy-X/ZeXTRa.

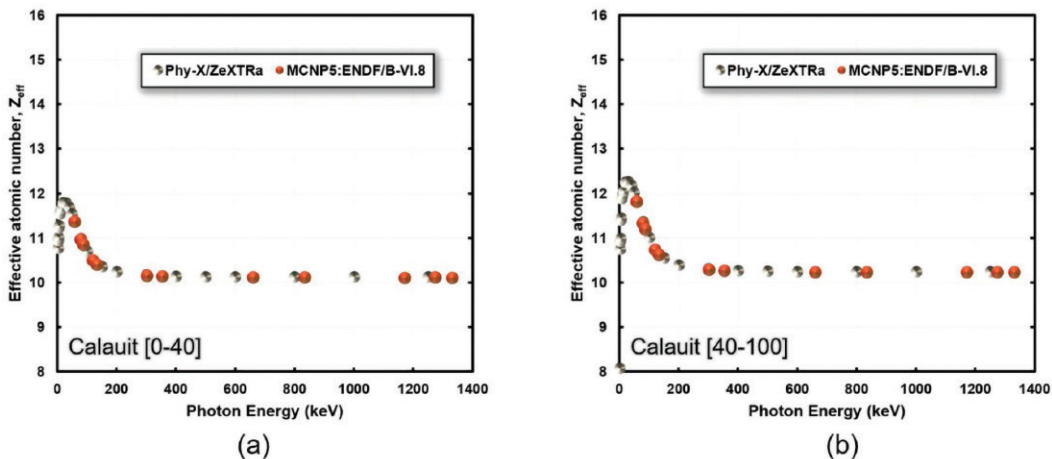


**Figure 5.**  $Z_{\text{eff}}$  values of mangrove soils from Calauit using MCNP5 and ENDF/B-VI.8 cross-sections and Phy-X/ZeXTRa.

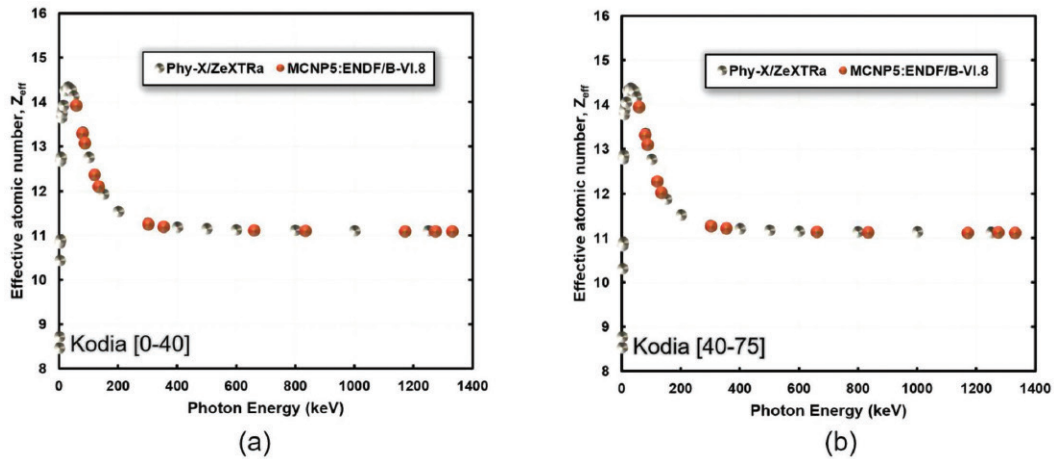


Figure 6.  $Z_{\text{eff}}$  values of mangrove soils from Kodia using MCNP5 and ENDF/B-VI.8 cross-sections and Phy-X/ZeXTRa.

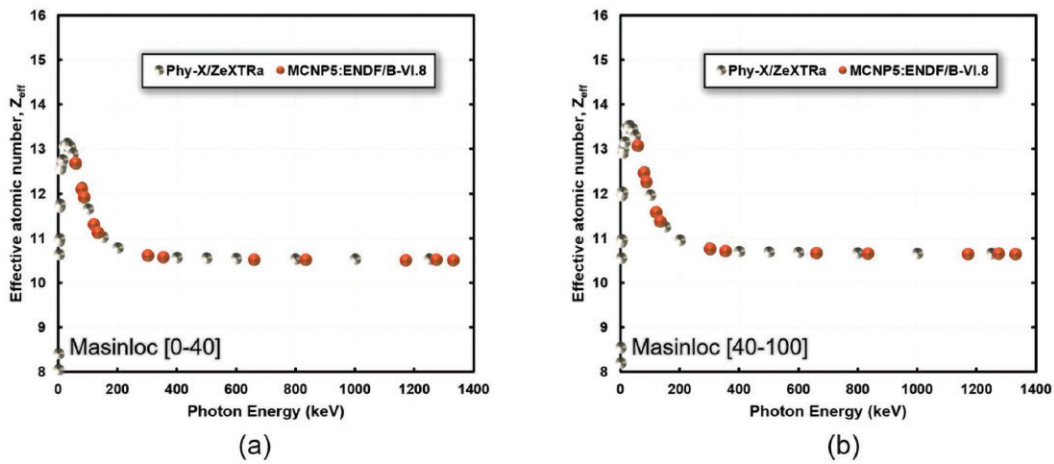


Figure 7.  $Z_{\text{eff}}$  values of mangrove soils from Masinloc using MCNP5 and ENDF/B-VI.8 cross-sections and Phy-X/ZeXTRa.

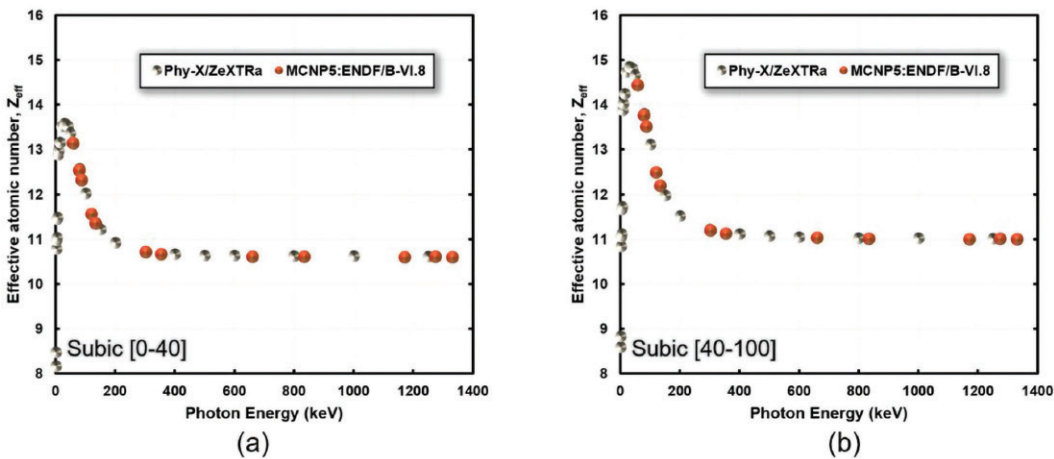


Figure 8.  $Z_{\text{eff}}$  values of mangrove soils from Subic using MCNP5 and ENDF/B-VI.8 cross-sections and Phy-X/ZeXTRa.

MCNP5 and PHITS codes were used to obtain the MAC values. The  $Z_{\text{eff}}$  values were obtained using logarithmic interpolation of the EPDL97 (ENDF/B-VI.8) photon cross-section library. The results for MAC values were found to be in good agreement with values generated by XCOM and by those described in the literature. The results for the  $Z_{\text{eff}}$  values were in good agreement with the results obtained with Phy-X/ZEXTRA program. Trends in all shielding parameters with respect to silica concentrations are presented. It was shown that increasing silica content has a negative correlation with  $Z_{\text{eff}}$  values. This correlation is attributed to the decreased proportion of heavier oxides as a consequence of the increase of silica. Additionally, this study emphasizes the use of the EPDL97 (ENDF/B-VI.8) library for obtaining  $Z_{\text{eff}}$  values using MAC values generated via the MC method, since this particular library is used by most photon transport codes.

## ACKNOWLEDGMENTS

The authors would like to acknowledge the DOST Philippines (through the Science Education Institute under the Human Resource Development Program) for the scholarship awarded to Mr. Frederick C. Hila. We also express our gratitude to Dr. Severino Salmo III for allowing us to use the samples of his project funded by the United States Agency for International Development through PEER (Partnership for Enhanced Engagement in Research) of the National Science Foundation (Project 3-191).

## REFERENCES

- AGAR O, TEKIN HO, SAYYED MI, KORKMAZ ME, CULFA O, ERTUGAY C. 2019. Experimental investigation of photon attenuation behaviors for concretes including natural perlite mineral. *Results Phys* 12: 237–243.
- AKAR TARIM U, GURLER O, OZMUTLU EN, YALCIN S. 2013. Monte Carlo calculations for gamma-ray mass attenuation coefficients of some soil samples. *Ann Nucl Energy* 58: 198–201.
- AKMAN F, TURAN V, SAYYED MI, AKDEMIR F, KAÇAL MR, DURAK R, ZAID MHM. 2019. Comprehensive study on evaluation of shielding parameters of selected soils by gamma and X-rays transmission in the range 13.94–88.04 keV using WinXCom and FFAST programs. *Results Phys* 15: 102751.
- AKMAN F, DURAK R, TURHAN MF, KAÇAL MR. 2015. Studies on effective atomic numbers, electron densities from mass attenuation coefficients near the

- K edge in some samarium compounds. *Appl Radiat Isot* 101: 107–113.
- AL-HADEETHI Y, AL-BURIAHI MS, SAYYED MI. 2020. Bioactive glasses and the impact of  $\text{Si}_3\text{N}_4$  doping on the photon attenuation up to radiotherapy energies. *Ceram Int* 46(4): 5306–5314.
- AL-MASRI MS, HASAN M, AL-HAMWI A, AMIN Y, DOUBAL AW. 2013. Mass attenuation coefficients of soil and sediment samples using gamma energies from 46.5 to 1332 keV. *J Environ Radioact* 116: 28–33.
- ALAM MN, MIAH MMH, CHOWDHURY MI, KAMAL M, GHOSE S, RAHMAN R. 2001. Attenuation coefficients of soils and some building materials of Bangladesh in the energy range 276–1332 keV. *Appl Radiat Isot* 54(6): 973–976.
- ALORFI HS, HUSSEIN MA, TIJANI SA. 2020. The use of rocks in lieu of bricks and concrete as radiation shielding barriers at low gamma and nuclear medicine energies. *Constr Build Mater* 251: 118908.
- APPOLONI CR, RIOS EA. 1994. Mass attenuation coefficients of Brazilian soils in the range 10–1450 keV. *Appl Radiat Isot* 45(3): 287–291.
- BERGER MJ, HUBBELL JH, SELTZER SM, CHANG J, COURSEY JS, SUKUMAR R, ZUCKER DS. 1998. XCOM: photon cross sections database. NIST Standard Reference Database.
- BOUKHRIS I, KEBAILI I, SAYYED MI, ASKIN A, RAMMAH YS. 2020. Linear, nonlinear optical and photon attenuation properties of  $\text{La}^{3+}$  doped tellurite glasses. *Opt Mater* 108: 110196.
- COSTA JC, BORGES JAR, PIRES LF. 2013. Soil bulk density evaluated by gamma-ray attenuation: Analysis of System Geometry. *Soil Tillage Res* 129: 23–31.
- DICEN GP, NAVARRETE IA, RALLOS RV, SALMO SG, GARCIA MCA. 2019. The role of reactive iron in long-term carbon sequestration in mangrove sediments. *J Soils Sediments* 19(1): 501–510.
- DIVINA R, SATHIYAPRIYA G, MARIMUTHU K, ASKIN A, SAYYED MI. 2020. Structural, elastic, optical and  $\gamma$ -ray shielding behavior of  $\text{Dy}^{3+}$  ions doped heavy metal incorporated borate glasses. *J Non-Cryst Solids* 545: 120269.
- ELIAS EA. 2004. A simplified analytical procedure for soil particle-size analysis by gamma-ray attenuation. *Comput Electron Agric* 42(3): 181–184.
- GERWARD L, GUILBERT N, JENSEN KB, LEVRING H. 2001. X-ray absorption in matter. *Reengineering XCOM. Radiat Phys Chem* 60(1–2): 23–24.

- GERWARD L, GUILBERT N, JENSEN KB, LEVRING H. 2004. WinXCom – a program for calculating X-ray attenuation coefficients. *Radiat Phys Chem* 71(3–4): 653–654.
- HAN I, DEMIR L, ŞAHİN M. 2009. Determination of mass attenuation coefficients, effective atomic and electron numbers for some natural minerals. *Radiat Phys Chem* 78(9): 760–764.
- HILA FC, AMORSOLO Jr. AV, JAVIER-HILA AMV, GUILLERMO NRD. 2020. A simple spreadsheet program for calculating mass attenuation coefficients and shielding parameters based on EPICS2017 and EPDL97 photoatomic libraries. *Radiat Phys Chem* 177: 109122.
- KUCUK N, TUMSAVAS Z, ÇAKIR M. 2013. Determining photon energy absorption parameters for different soil samples. *J Radiat Res* 54(3): 578–586.
- MAHMOUD KA, SAYYED MI, TASHLYKOV OL. 2019a. Comparative studies between the shielding parameters of concretes with different additive aggregates using MCNP-5 simulation code. *Radiat Phys Chem* 165: 108426.
- MAHMOUD KA, SAYYED MI, TASHLYKOV OL. 2019b. Gamma ray shielding characteristics and exposure buildup factor for some natural rocks using MCNP-5 code. *Nucl Eng Technol* 51(7): 1835–1841.
- MEDHAT ME. 2012. Application of gamma-ray transmission method for study the properties of cultivated soil. *Ann Nucl Energy* 40(1): 53–59.
- MEDHAT ME. 2015. Comprehensive study of photon attenuation through different construction matters by Monte Carlo simulation. *Radiat Phys Chem* 107: 65–74.
- MEDHAT ME, DEMIR N, AKAR TARIM U, GURLER O. 2014. Calculation of gamma-ray mass attenuation coefficients of some Egyptian soil samples using Monte Carlo methods. *Radiat Eff Defects Solids* 169(8): 706–714.
- MONISHA M, D’SOUZAAN, HEGDE V, PRABHU NS, SAYYED MI, LAKSHMINARAYANA G, KAMATH SD. 2020. Dy<sup>3+</sup> doped SiO<sub>2</sub>-B<sub>2</sub>O<sub>3</sub>-Al<sub>2</sub>O<sub>3</sub>-NaF-ZnF<sub>2</sub> glasses: an exploration of optical and gamma radiation shielding features. *Curr Appl Phys* 20(11): 1207–1216.
- MUDAHAR GS, SAHOTA HS. 1988a. Soil: A radiation shielding material. *Int J Radiat Appl Instrum Part* 39(1): 21–24.
- MUDAHAR GS, SAHOTA HS. 1988b. Effective atomic number studies in different soils for total photon interaction in the energy region 10–5000 keV. *Int J Radiat Appl Instrum Part* 39(12): 1251–1254.
- OBAID SS, GAIKWAD DK, PAWAR PP. 2018a. Determination of gamma ray shielding parameters of rocks and concrete. *Radiat Phys Chem* 144: 356–360.
- OBAID SS, SAYYED MI, GAIKWAD DK, PAWAR PP. 2018b. Attenuation coefficients and exposure buildup factor of some rocks for gamma ray shielding applications. *Radiat Phys Chem* 148: 86–94.
- OBAID SS, SAYYED MI, GAIKWAD DK, TEKIN HO, ELMAHROUG Y, PAWAR PP. 2018c. Photon attenuation coefficients of different rock samples using MCNPX, Geant4 simulation codes and experimental results: a comparison study. *Radiat Eff Defects Solids* 173(11–12): 900–914.
- ÖZPOLAT F, ALIM B, ŞAKAR E, BÜYÜKYILDIZ M, KURUDIREK M. 2020. Phy-X/ZeXTRa: a software for robust calculation of effective atomic numbers for photon, electron, proton, alpha particle, and carbon ion interactions. *Radiat Environ Biophys* 59: 321–329.
- PIRES LF. 2018. Soil analysis using nuclear techniques: A literature review of the gamma ray attenuation method. *Soil Tillage Res.* 184: 216–234.
- ŞAKAR E, ÖZPOLAT ÖF, ALIM B, SAYYED MI, KURUDIREK M. 2020. Phy-X / PSD: Development of a user friendly online software for calculation of parameters relevant to radiation shielding and dosimetry. *Radiat Phys Chem* 166: 108496.
- SATO T, IWAMOTO Y, HASHIMOTO S, OGAWA T, FURUTA T, ABE SI, KAI T, TSAI PE, MATSUDAN, IWASE H, SHIGYO N, SIHVER L, NIITA K. 2018. Features of particle and heavy ion transport code system (PHITS) version 3.02 [User Version 3.17]. *J Nucl Sci Technol* 3131: 1–7.
- SAYYED MI, AKMAN F, TURAN V, ARAZ A. 2019. Evaluation of radiation absorption capacity of some soil samples. *Radiochim Acta* 107(1): 83–93.
- SHARIFI S, BAGHERI R, SHIRMARDI SP. 2013. Comparison of shielding properties for ordinary, barite, serpentine and steel-magnetite concretes using MCNP-4C code and available experimental results. *Ann Nucl Energy* 53: 529–534.
- SINGH T, KAUR P, SINGH PS. 2007. A study of photon interaction parameters in some commonly used solvents. *J Radiol Prot* 27(1): 79–85.
- SINGH VP, KORKUT T, BADIGER NM. 2018. Comparison of mass attenuation coefficients of concretes using FLUKA, XCOM and experiment results. *Radioprotection* 53(2): 145–148.

- TAQIAH, KHALIL HJ. 2017. An investigation on gamma attenuation of soil and oil-soil samples. *J Radiat Res and Applied Sciences* 10(3): 252–261.
- TAQI AH, AL NUAIMY QAM, KAREM GA. 2016. Study of the properties of soil in Kirkuk, Iraq. *J Radiat Res and Applied Sciences* 9(3): 259–265.
- UNA, SAHIN Y. 2011. Determination of mass attenuation coefficients, effective atomic and electron numbers, mean free paths and kermas for PbO, barite and some boron ores. *Nucl Instrum Methods Phys Res, Sect B* 269(13): 1506–1511.
- UNA, SAHIN Y. 2012. Determination of mass attenuation coefficients, effective atomic numbers, effective electron numbers and kermas for Earth and Martian soils. *Nucl Instrum Methods Phys Res, Sect B* 288: 42–47.
- X-5 MONTE CARLO TEAM. 2008. MCNP – Version 5, Vol. I: Overview and Theory, LA-UR-03-1987.